

Partially coherent self-similar pulses in resonant linear absorbers

L. Mokhtarpour, G. H. Akter, and S. A. Ponomarenko*

Department of Electrical and Computer Engineering, Dalhousie University,
Halifax, NS, B3J 2X4 Canada

*serpo@dal.ca

Abstract: We theoretically describe several classes of ultrashort partially coherent pulses that maintain their shape on propagation in coherent linear absorbers near optical resonance.

© 2012 Optical Society of America

OCIS codes: (030.0030) Coherence and statistical optics; (320.0320) Ultrafast optics; (320.5550) Pulses.

References and links

1. G. P. Agrawal, *Fiber-Optic Communication Systems*, 3rd ed. (Wiley, 2002).
2. M. Bertolotti, A. Ferrari, and L. Sereda, "Coherence properties of nonstationary polychromatic light sources," *J. Opt. Soc. Am. B* **12**, 341–347 (1995).
3. L. Sereda, M. Bertolotti, and A. Ferrari, "Coherence properties of nonstationary light wave fields," *J. Opt. Soc. Am. B* **15**, 695–705 (1998).
4. P. Pääkkönen, J. Turunen, P. Vahimaa, A. T. Friberg, and F. Wyrowski, "Partially coherent Gaussian pulses," *Opt. Commun.* **204**, 53–58 (2002).
5. H. Lajunen, J. Tervo, J. Turunen, P. Vahimaa, and F. Wyrowski, "Spectral coherence properties of temporarily modulated stationary light sources," *Opt. Express* **11**, 1894–1899 (2003).
6. S. A. Ponomarenko, G. P. Agrawal, and E. Wolf, "Energy spectrum of a nonstationary ensemble of pulses," *Opt. Lett.* **29**, 394–396 (2004).
7. B. Davis, "Measurable coherence theory for statistically periodic fields," *Phys. Rev. A* **76**, 043843 (2007).
8. P. Vahimaa and J. Turunen, "Independent-elementary-pulse representation for non-stationary fields," *Opt. Express* **14**, 5007–5012 (2006).
9. A. T. Friberg, H. Lahunen, and V. Torres-Company, "Spectral elementary-coherence-function representation for partially coherent light pulses," *Opt. Express* **15**, 5160–5165 (2007).
10. S. A. Ponomarenko, "Complex Gaussian representation of statistical pulses," *Opt. Express* **19**, 17086–17091 (2011).
11. Q. Lin, L. Wang, and S. Zhu, "Partially coherent light pulse and its propagation," *Opt. Commun.* **219**, 65–70 (2003).
12. M. Brunel and S. Coëtlemec, "Fractional-order Fourier formulation of the propagation of partially coherent light pulses," *Opt. Commun.* **230**, 1–5 (2004).
13. E. Wolf, *Introduction to the Theory of Coherence and Polarization* (Cambridge University Press, 2007).
14. S. A. Ponomarenko, "Degree of phase-space separability of statistical pulses," *Opt. Express* **20**, 2548–2555 (2012).
15. H. Lajunen, V. Torres-Company, J. Lancis, E. Silvestre, and P. Andrés, "Pulse-by-pulse method to characterize partially coherent pulse propagation in instantaneous nonlinear media," *Opt. Express* **18**, 14979–14991 (2011).
16. S. Haghgoo and S. A. Ponomarenko, "Self-similar pulses in coherent linear amplifiers," *Opt. Express* **19**, 9750–9758 (2011).
17. S. Haghgoo and S. A. Ponomarenko, "Shape-invariant pulses in resonant linear absorbers," *Opt. Lett.* **37**, 1328–1330 (2012).
18. L. Mandel and E. Wolf, *Optical Coherence and Quantum Optics* (Cambridge University Press, 1995).
19. H. Lajunen, J. Tervo, and P. Vahimaa, "Overall coherence and coherent-mode expansion of spectrally partially coherent plane-wave pulses," *J. Opt. Soc. Am. A* **21**, 2117–2123 (2004).
20. P. W. Milonni and J. H. Eberly, *Lasers* (Wiley, 1985).
21. M. Abramowitz and I. A. Stegun, *Handbook of Mathematical Functions* (Dover, 1972).

1. Introduction

The growing interest in the ultrafast optical communication systems [1] has motivated the recent surge of activity in the field of ultrafast statistical optics [2–12]. The progress was initiated by the pioneering work [2, 3] that extended the optical coherence theory of statistically stationary fields [13] to the non-stationary case.

To date, a good deal of attention has been paid to modeling realistic partially coherent sources [4, 5], the search for an adequate definition of statistical pulse spectrum [6] and for a measurable theory of random pulses [7] as well as the advancement of various statistical representations thereof [8–10]. Propagation properties of statistical pulses—especially the ones that maintain their temporal profile on propagation—have also been explored in linear [11, 12, 14] and nonlinear [15] dispersive media far from internal resonances. Although shape-invariant propagation of fully coherent ultrashort pulses in linear amplifiers and absorbers in the vicinity of an optical resonance has been recently examined [16, 17], the influence of statistical properties on pulse evolution has not yet been explored in the resonant case.

The objective of this work is to present explicit classes of partially coherent pulses that propagate in resonant linear absorbers without changing their shape. We show how such pulses can be constructed from the previously discovered shape-invariant modes of resonant absorbers by extending the coherent-mode representation of optical coherence theory [18] to the case of statistical pulses in a manner similar to [19].

2. Partially coherent self-similar pulses in coherent linear absorbers

To set the stage, we examine small-area statistical pulse propagation in a homogeneously broadened resonant absorber under exact resonance condition: the pulse carrier frequency coincides with a resonant transition frequency of the medium atoms. A dilute atomic vapor filling a high-vacuum cell can serve as a physical realization of the medium. To eliminate inhomogeneous broadening, we assume the atomic velocities to be well collimated orthogonally to the input laser beam such that no Doppler broadening takes place.

To illustrate a typical experimental situation, we consider a dilute sodium vapor with the density $N \sim 10^{11} \text{ cm}^{-3}$ at room temperature at the pressure of $P = 0.1$ Torr, say. One can then estimate a characteristic spectral width due to collision broadening as $\delta\nu_c \sim 10^3$ MHz [20]. Assuming further that dipole relaxation is mainly due to collisions, we can estimate a typical dipole relaxation time, $T_\perp \sim \delta\nu_c^{-1} \sim 10^{-9}$ s. It follows that the linear absorption length of this system can be estimated as $L_A = \alpha^{-1} \simeq 2$ mm, where $\alpha = NT_\perp e^2 / 2\epsilon_0 mc$ is a small-signal absorption coefficient. Thus, the proposed self-similar pulses can be realized with nanosecond small-area input pulses in a few-centimeter long cell filled with the homogeneously broadened dilute vapor.

Next, we recall that the system supports a class of fully coherent shape-invariant modes; the spectral profile of each mode is given by [17]

$$\tilde{\mathcal{E}}_s(\omega, \zeta) \propto \frac{(\alpha\zeta_0/2)^s}{(1 - i\omega T_\perp)^{s+1}} \exp\left[-\frac{\alpha(\zeta + \zeta_0)}{2(1 - i\omega T_\perp)}\right]. \quad (1)$$

Here α is a small-signal inverse absorption length, T_\perp is an individual dipole relaxation time, and ζ_0 determines the spectral mode profile at the source. Introducing dimensionless variables $\Omega = \omega T_\perp$ and $Z = \alpha\zeta$ and restricting ourselves to the integer index modes ($s = n$), we can rewrite the spectral field amplitude of each shape-invariant mode in the form

$$\tilde{\mathcal{E}}_n(\Omega, Z) \propto \frac{(Z_0/2)^n}{(1 - i\Omega)^{n+1}} \exp\left[-\frac{Z + Z_0}{2(1 - i\Omega)}\right]. \quad (2)$$

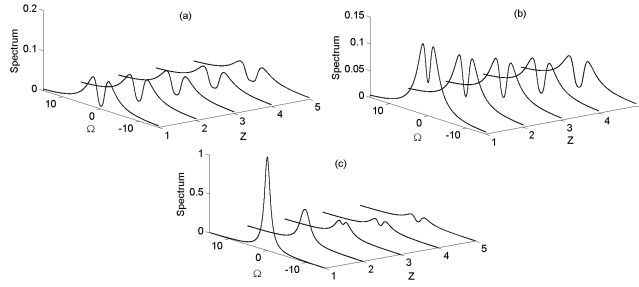


Fig. 1. Spectral amplitude of the pulse with the power-law modal weight distribution in arbitrary units. The parameters are (a) $\lambda = 0.1$, $Z_0 = 5$; (b) $\lambda = 0.3$, $Z_0 = 3$, and (c) $\lambda = 10$, $Z_0 = 0.1$.

Any partially coherent shape-invariant pulse can be expressed as a linear superposition of shape-invariant modes with random coefficients as

$$\tilde{\mathcal{E}}(\Omega, Z) = \sum_{n=0}^{\infty} C_n \tilde{\mathcal{E}}_n(\Omega, Z). \quad (3)$$

In Eq. (3), the coefficients determine the statistics of the source viz.,

$$\langle C_n^* C_m \rangle = \lambda_n \delta_{mn}, \quad (4)$$

where $\lambda_n \geq 0$ and the angle brackets indicate ensemble averaging. The second-order statistical properties of pulses in the spectral domain are described by the cross-spectral density distribution defined as

$$W(\Omega_1, \Omega_2, Z) = \langle \tilde{\mathcal{E}}^*(\Omega_1, Z) \tilde{\mathcal{E}}(\Omega_2, Z) \rangle. \quad (5)$$

It follows from Eqs. (4) and (5) that the cross-spectral density can then be expressed as a Mercer-type series in the form [18]

$$W(\Omega_1, \Omega_2, Z) = \sum_{n=0}^{\infty} \lambda_n \tilde{\mathcal{E}}_n^*(\Omega_1, Z) \tilde{\mathcal{E}}_n(\Omega_2, Z). \quad (6)$$

Although a multitude of partially coherent shape-invariant pulses can be represented by the expansion (6), closed-form results can only be obtained for a few classes of pulses. In the following sections we consider two such cases.

3. Pulses with the power-law distribution of modal weights

First, assume the modal weights $\{\lambda_n\}$'s have a power distribution:

$$\lambda_n = \mathcal{A} \lambda^{2n}, \quad (7)$$

where $\mathcal{A} > 0$ is a normalization constant specifying the overall intensity of a partially coherent pulse, and $\lambda \geq 0$. It follows at once from Eqs. (2), (6), and (7) that the spectrum of the pulse, defined as $S(\Omega, Z) \equiv W(\Omega, \Omega, Z)$ [6], is

$$S(\Omega, Z) = \frac{\mathcal{A}}{(1 - \lambda^2 Z_0^2/4) + \Omega^2} \exp\left[-\frac{Z + Z_0}{1 + \Omega^2}\right]. \quad (8)$$

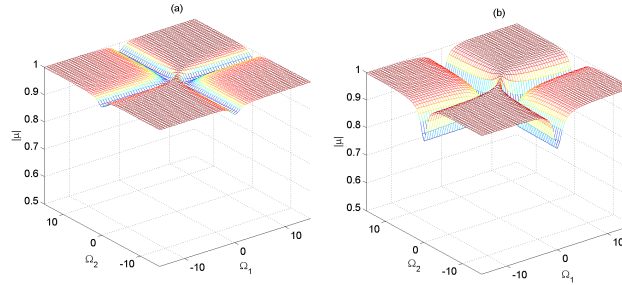


Fig. 2. Modulus of the spectral degree of coherence. The parameters are (a) $\lambda = 0.1$, $Z_0 = 5$ and (b) $\lambda = 10$, $Z_0 = 0.1$.

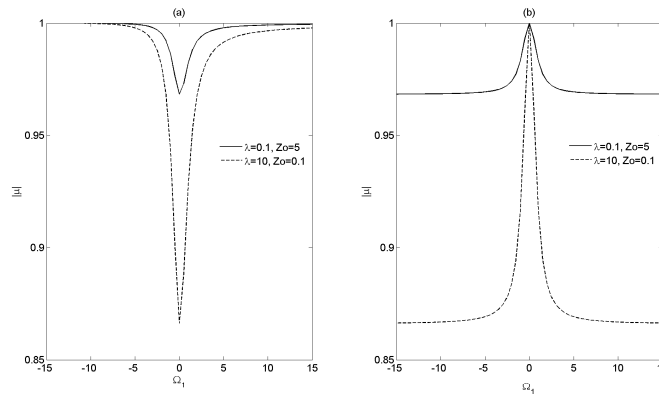


Fig. 3. Modulus of the spectral degree of coherence as a function of Ω_1 for a fixed Ω_2 : (a) $\Omega_2 = -15$, (b) $\Omega_2 = 0$.

Equation (8) corresponds to a physical pulse spectrum only if the constraint $0 \leq \lambda < 2/Z_0$ is imposed. The latter is rather stringent as it stipulates that λ be fairly small for sufficiently large Z_0 . Notice also that the spectrum (8) has the shape reminiscent of the zero-index mode spectrum $|\mathcal{E}_0(\Omega, Z)|^2$ of Ref. [17], though its peak amplitude is scaled by the factor of $(1 - \lambda^2 Z_0^2/4)^{-1}$.

Further analysis reveals that the shape of the pulse spectrum depends on the magnitude of two parameters: λ and Z_0 . In particular, the pulse spectrum at the source can have either a hole, or a dip, or else a peak at the center, depending on λ and Z_0 . The situation is illustrated in Fig. 1 where the pulse spectrum evolution is displayed for three sets of parameters: (a) $\lambda = 0.1$, $Z_0 = 5$; (b) $\lambda = 0.3$, $Z_0 = 3$, and (c) $\lambda = 10$, $Z_0 = 0.1$. As is seen in Fig. 1(a), the spectrum with a hole at the center propagates in a self-similar fashion from the outset. Whenever there is only a dip at the center of the incident pulse—as is shown in Fig. 1(b)—the dip deepens on propagation until a hole is burnt at the center and the pulse enters its self-similar evolution stage. If, on the other hand, the spectrum has a central peak (see Fig. 1(c)), the latter eventually transforms into a hole with the subsequent self-similar pulse evolution.

Coherence properties of the pulse are described by the spectral degree of coherence defined

as [18]

$$\mu(\Omega_1, \Omega_2, Z) = \frac{W(\Omega_1, \Omega_2, Z)}{\sqrt{S(\Omega_1, Z)}\sqrt{S(\Omega_2, Z)}}. \quad (9)$$

The latter can be worked out analytically, but the resulting expression is rather cumbersome. Instead, we exhibit the magnitude of the spectral degree of coherence in the source plane in Fig. 2 for two sets of parameters: (a) $\lambda = 0.1$, $Z_0 = 5$ and (b) $\lambda = 10$, $Z_0 = 0.1$. As is seen in the figure, the spectral coherence properties of the pulses are nonuniform and dependent on the values of parameters. To illustrate these points, we display in Fig. 3 $|\mu|$ as a function of Ω_1 , say, for fixed Ω_2 . It is seen in the figure that the degree of coherence can have a local maximum or minimum at the center, $\Omega_1 = 0$, depending on the position of the other spectral point. The magnitudes of the maxima and minima depend on the values of the other parameters.

4. Pulses with modal weight distributions decaying faster than the power-law

Next, we examine the following modal weight distribution,

$$\lambda_n = \mathcal{B} \frac{\lambda^{2n}}{(n!)^2}, \quad (10)$$

\mathcal{B} being a positive normalization constant. It can be inferred from Eqs. (2), (6), and (10) using the representation for the zero-order modified Bessel function [21],

$$I_0(x) = \sum_{n=0}^{\infty} \frac{(x/2)^{2n}}{(n!)^2}, \quad (11)$$

that the partially coherent pulse spectrum in the case takes the form

$$S(\Omega, Z) = \frac{\mathcal{B}}{1 + \Omega^2} I_0\left(\frac{\lambda Z_0}{\sqrt{1 + \Omega^2}}\right) \exp\left[-\frac{Z + Z_0}{1 + \Omega^2}\right]. \quad (12)$$

We conclude by examining Eq. (12) that provided $\lambda < 1$, the spectral hole or dip presence at the pulse center in the source plane depends on the values of λ and Z_0 . However, unlike in the previously considered case, if $\lambda > 1$, there can be no spectral hole at the source.

We illustrate these observations by exhibiting the pulse spectrum of Eq. (12) in Fig. 4 for four sets of parameters: (a) $\lambda = 0.9$, $Z_0 = 0.1$; (b) $\lambda = 0.9$, $Z_0 = 15$; (c) $\lambda = 2$, $Z_0 = 0.1$, and (d) $\lambda = 2$, $Z_0 = 15$. It is seen by comparing Figs. 4(a) and 4(c) that for sufficiently small $Z_0 = 0.1$, there is a peak at the center in the source plane in both figures. At the same time, as Z_0 increases to 15, say, a hole is formed at the center for $\lambda = 0.9 < 1$ as is seen in Fig. 4(b). Yet, the pulse spectrum has a peak at the center for $\lambda = 2 > 1$ as shown in Fig. 4(d). Our numerical simulations indicate that no matter how close the value of λ approaches unity from the above, only a dip but not a hole can be formed at the center of the pulse spectrum.

In Fig. 5, we also present the corresponding spectral degree of coherence in the source plane for $Z_0 = 15$ with $\lambda = 0.9$ (left) and $\lambda = 2$ (right). Note that there is no constraint on the magnitude of λ in Eq. (12) which makes this class of pulses wider than the previously considered one. On comparing Fig. 2 and Fig. 5, we observe that first, the spectral degree of coherence is rotationally symmetric in the former figure while the rotational symmetry is broken in the latter. Second, we notice that the quantitative dependence of $|\mu|$ on the parameters is stronger for the second class of pulses than is for the first. To bring these points home, we exhibit in Fig. 6 the cross-sectional plot of $|\mu|$ for a couple fixed values of one of the frequencies, $\Omega_2 = -15$ in Fig. 6(a) and $\Omega_2 = 0$, in Fig. 6(b). On comparing Figs. 3 and 6, we can see that not only does the qualitative behavior of $|\mu|$ richer in Fig. 6, but pulse coherence properties can be tuned within a wider range for the second class of pulses than for the first one.

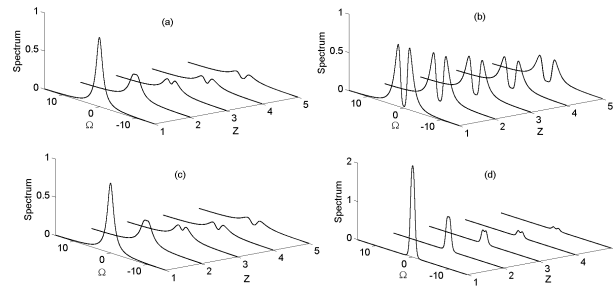


Fig. 4. Spectral amplitude of the pulse with $\lambda_n \propto \lambda^{2n}/(n!)^2$ in arbitrary units. The parameters are (a) $\lambda = 0.9, Z_0 = 0.1$; (b) $\lambda = 0.9, Z_0 = 15$; (c) $\lambda = 2, Z_0 = 0.1$, and (d) $\lambda = 2, Z_0 = 15$.

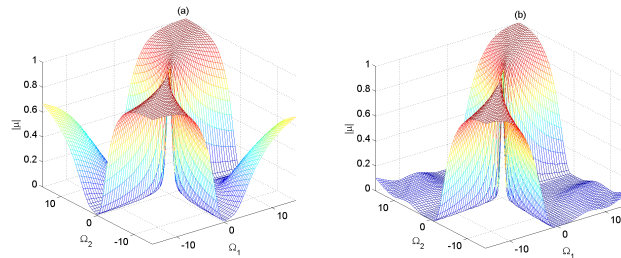


Fig. 5. Modulus of the spectral degree of coherence. The parameters are (a) $\lambda = 0.9, Z_0 = 15$ and (b) $\lambda = 2, Z_0 = 15$.

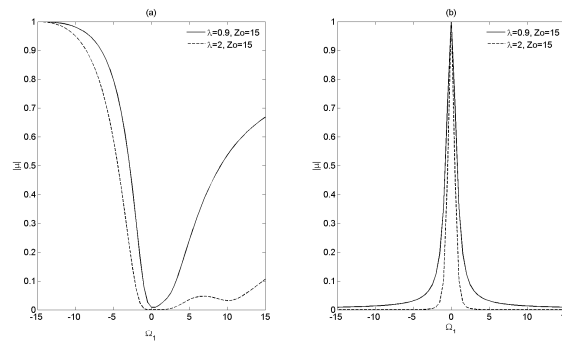


Fig. 6. Modulus of the spectral degree of coherence as a function of Ω_1 for a fixed Ω_2 : (a) $\Omega_2 = -15$, (b) $\Omega_2 = 0$.

In conclusion, we have theoretically described several classes of partially coherent self-similar pulses. We found closed form expressions for two-time correlation functions fully describing second-order statistical properties of the pulses. We also explored coherence properties of the new pulses and shown that, in general, the pulse coherence properties are highly nonuni-

form across the their temporal profiles. The spectral profiles of the new pulses may have a spectral hole or a dip which can affect their short-distance evolution; however the long-term evolution is self-similar in either case.